Anisotropic localized surface plasmon resonances in CuS nanoplates prepared by size-selective precipitation

Yasushi Hamanaka[1*], Kaoru Yamada[1], Tatsunori Hirose[1], and Toshihiro Kuzuya[2]

[1]*Department of Physical Science and Engineering, Nagoya Institute of Technology, Nagoya 466-8555, Japan*
[2]*College of Design and Manufacturing Technology, Muroran Institute of Technology, Muroran, Hokkaido 052-8585, Japan*

[*]E-mail: hamanaka@nitech.ac.jp

CuS nanoplates were synthesized by a colloidal method and separated into four fractions of nanoplates with different aspect ratios by a size-selective precipitation. In addition to a strong near infrared absorption band ascribed to the in-plane mode of the localized surface plasmon resonance (LSPR), we found a weak absorption band on the high frequency tail of the in-plane LSPR band. The frequency of the weak absorption band was almost constant and independent of the aspect ratio, while the in-plane LSPR band exhibited a strong aspect ratio dependence. These characteristics suggested that the weak absorption band is ascribed to the out-of-plane LSPR. Although the out-of-plane LSPR was expected to be difficult to observe for CuS nanoplates due to its low intensity and overlap with the strong in-plane resonance, we could successfully identify the out-of-plane mode by reducing the width of the size distribution and spectral broadening caused thereby.

1. Introduction

Localized surface plasmon resonance (LSPR) is a characteristic optical behavior observed in metal nanosystems.[1] LSPR in nanoparticles of noble metals such as gold and silver has been studied for more than a century; for instance, Faraday's study on "ruby gold" was carried out in the middle of the 19th century,[2] and Mie studied the optical properties of gold particles at the beginning of the 20th century.[3] Recent developments in the research of LSPR are driven by the proposal of "plasmonics", in which a dramatically improved efficiency of light-matter interactions due to LSPR-induced strong near-field effects has attracted attention.[4,5] Thus, plasmonics is believed to have great potential for various photonic applications. In the past few years, LSPR of non-metallic nanomaterials, especially of semiconductor nanoparticles, has also attracted much attention because of several advantages over metal nanoparticles.[6-10] Semiconductor nanoparticles exhibit tunable LSPRs over a wide frequency region from near infrared (NIR) to mid-infrared, which arise from carrier doping. In contrast, LSPR of metal nanoparticles is limited to the visible region, and frequency-tuning can be achieved by controlling size and shape of these nanoparticles.[1,4,5] Plasmonic properties in the NIR region of doped semiconductor nanoparticles have promising biological applications, e.g., bioimaging, biosensing, and photothermal therapy, because they operate in an optical window where the living body is transparent.[11,12] In addition, excellent plasmonic responses in the NIR are suitable for photonic devices used for optical fiber communications as there exist telecom frequencies in this spectral region.

Copper chalcogenides (Cu_xS, Cu_xSe, and Cu_xTe,) are the most widely studied materials as plasmonic semiconductor nanoparticles, because they can be easily synthesized by simple colloidal methods.[6,8,11-13] Copper chalcogenides are self-doped semiconductors where copper deficiencies lead to the formation of holes at the top of the valence band.[14,15] Anisotropic nanoparticles of copper chalcogenides with plate-like shapes as well as isotropic spherical nanoparticles have been synthesized, and their fundamental spectroscopic and plasmonic properties have been investigated.[12,16-20] In contrast to spherical nanoparticles, the nanoparticles with anisotropic shape exhibited splitting of the LSPR band which, in many previous reports, has been experimentally observed in metallic nanoparticles, such as gold and silver nanorods and nanodisks.[21,22] Such a mode splitting originates in a directional

difference in the resonant frequencies of the collective oscillation of the free carriers due to the anisotropic nature of the nanorods and nanodisks. However, mode splitting of the LSPR band has rarely been observed for semiconductor nanoparticles. In most studies on the LSPR of anisotropic semiconductor nanoparticles such as nanoplates, nanorods, nanocubes, and tetrapods, single broad absorption peaks are detected and identified as the LSPR bands.[12,13,17-20,23] In the case of nanoplates, such peaks are assigned to the in-plane dipolar LSPR mode. Theoretical simulations of the extinction spectra of Cu_xS nanoplates predict that a significantly weaker, out-of-plane, dipolar LSPR band is present on the high frequency tail of the in-plane band;[19] however, it is difficult to resolve the out-of-plane mode, due to its weak extinction cross-section and overlap with the strong in-plane LSPR band.[19,20] Moreover, inhomogeneous broadening due to size dispersity can hide a weak out-of-plane peak. Two distinct absorption peaks in the NIR are observed for Cu_2S nanodisks by Tao et al. and claimed to be in-plane and out-of-plane dipolar LSPRs;[16] however, we consider that such an assignment of the LSPR mode is questionable because there are some discrepancies between their spectral characteristics and both the theoretical predictions and the experimental observations for LSPRs in other nanoplates. First, they report that the intensity of the in-plane band is lower than that of the out-of-plane band, despite the in-plane band being 10 times stronger than the out-of-plane band in silver nanoplates[24] and a similar tendency being predicted for Cu_xS nanoplates by theoretical calculations, as discussed above.[19] Secondly, the aspect ratio dependence of the frequencies of the out-of-plane mode is larger than that of the in-plane mode; however, this is the opposite behavior to the LSPRs of the nanoplates. Both experimental and theoretical studies of silver nanoplates and a theoretical study of Cu_xS nanoplates have reported that the apparent frequency shift is observed only in the in-plane mode.[20,25] Finally, the spectral width of the out-of-plane band is over three times larger than that of the in-plane band in Tao's report, while the in-plane band is slightly broader in metal nanoplates.[16,24] Therefore, observation of the out-of-plane LSPR in non-spherical semiconductor nanoparticles is still a controversial issue.

In this study, we investigated the splitting of the absorption band of the LSPR due to the anisotropic shape of copper sulfide (CuS) nanoplates. Besides a dominant LSPR band ascribed to the in-plane mode, a weak absorption band was successfully observed in CuS nanoplates having a narrow particle size distribution due to preparation by a size-selective

precipitation technique. We could reveal that this weak absorption band was attributed to the out-of-plane LSPR based on spectral aspects which are observed in nanoplates of Au and Ag, but rarely in semiconductor systems.[25]

2. Experimental methods

CuS nanoplates were synthesized via a solution route developed for copper-alkylamine complexes. We mixed 0.4 mmol of copper acetate with octhylamine in toluene. After the solution was heated up to 363 K and stirred under an inert atmosphere for 30 min, 0.8 mmol of sulfur powder dissolved in oleylamine was rapidly injected into the former solution. Then, the mixture was stirred for 30 min and subsequently cooled down to room temperature. At this stage, CuS nanoplates with an average in-plane diameter of ~10 nm and a thickness of ~4 nm were obtained. To obtain CuS nanoplates with a narrow size distribution, we used size-selective precipitation method which has been widely used for the isolation of monodisperse colloidal nanoparticles of semiconductors and metals.[26,27] Precipitates obtained after the addition of a small amount of acetone (non-solvent) to a crude solution of the nanoplates were separated from the soluble fractions by centrifugation. Then, acetone was added to the supernatant and precipitates were isolated again. This procedure was repeated until no further precipitates were formed. Finally, we could separate the mixtures of crude nanoplates into four fractions of nanoplates denoted as S1-S4. Each fraction was re-dispersed in hexane.

The size and shape of individual nanoplates were determined using a transmission electron microscope (TEM; Hitachi HF-2000). The crystal structure was investigated by X-ray diffraction (XRD) using a powder diffractometer (MAC Science M18XCE) with Cu-Kα radiation. An elemental analysis of the nanoplates was carried out using energy-dispersive X-ray spectroscopy (EDX; Horiba EMAX-7000). Absorption spectra of the nanoplates were measured by a standard double-beam spectrophotometer (JASCO V-570).

3. Results and discussion

Figures 1(a)–1(d) and 1(e) show TEM images of CuS nanoplates S1 to S4 and an XRD pattern of as-synthesized nanoplates before the size-selective treatment, respectively. The two-dimensional morphology of the nanoplates can be clearly seen in the TEM images of

each sample. The XRD pattern indicates that the nanoplates have a hexagonal CuS structure (covellite). The presence of the hexagonal CuS structure was supported by the results of the elemental analysis. The ratios of Cu to S, i.e., Cu/S, were determined to be 0.81, 0.81, 0.75, and 0.72 for nanoplates S1, S2, S3, and S4, respectively, indicating slight Cu deficiency compared to stoichiometric CuS. From the TEM images in Figs. 1(a)–1(d), the average in-plane diameters, D, of nanoplates S1–S4 were estimated to be 17.1 ± 1.8, 13.5 ± 1.8, 11.6 ± 1.5, and 8.7 ± 1.8 nm, respectively. The thickness of the nanoplates, t, was about 5 nm for S1 and 4 nm for S2–S4. Thus, aspect ratios (i.e., the ratio between the thickness and in-plane diameter) of nanoplates S1–S4 were about $t/D = 0.29$, 0.30, 0.35, and 0.46. This result indicates that the size-separation of the CuS nanoplates was successfully accomplished by the precipitation and re-dispersion method.

Figure 2(a) shows absorption spectra of the size-selected CuS nanoplates S1–S4. A broad absorption peak due to LSPR can be seen around 0.8–1.3 eV in each sample. The absorption peak exhibits a blue-shift as the nanoplate diameter D decreases (aspect ratio t/D increases). Due to the anisotropic structure of the nanoplates, in-plane and out-of-plane modes of the LSPR are expected to have different frequencies.[1] However, only the in-plane mode was observed for CuS nanoplates, because the out-of-plane mode may be comparatively weak as could be expected from the results of silver and gold nanoplates and also from simulations of CuS nanoplates.[19,20,28] Therefore, absorption peaks around 0.8–1.3 eV can be attributed to the in-plane mode of the dipolar LSPR, which has been reported for CuS nanoplates and nanodisks in several previous studies.[12,16,17,19,20,28] A clear blue-shift depending on the aspect ratios is also characteristic of the in-plane mode.[19,20] Figure 2(b) shows the FWHM of these absorption bands plotted versus the reciprocal diameter ($1/D$). We can see a linear dependence of the FWHM on $1/D$ where the FWHM decreases with an increase of D. This observation can be ascribed to the effect of a limited mean-free-path of free carriers, which is described in detail later.

Another noteworthy feature of these absorption spectra is the very weak spectral component existing around 2 eV which overlapped with the tail of the intense in-plane mode. According to earlier studies on the LSPR in metal nanoplates, the frequency of the out-of-plane mode of the dipolar LSPR is higher compared with that of the in-plane mode, while the out-of-plane absorbance is much weaker than that of the in-plane mode.[19,20,22,28]

Numerical simulation of extinction spectra of CuS nanoplates by the discrete dipole approximation also displays a strong in-plane mode and a weak peak, originating from the out-of-plane mode, on the high frequency side of the in-plane mode.[19] The whole spectral shape closely resembles those observed in this study. Such characteristics suggest that the weak features around 2 eV may be attributed to the out-of-plane resonance. In order to examine the weak spectral components closely, the same absorption spectra as in Fig. 2(a) are displayed again on a logarithmic scale in Fig. 3(a). In these spectra, the relevant spectral features, which are labeled by the arrow, can be observed more clearly. Figures 3(b)–3(e) show the secondary differential spectra of nanoplates S1–S4 calculated from the corresponding absorption spectra. Each differential spectrum shows a dip around 2 eV, clearly indicating the presence of an additional absorption peak. The inset of Fig. 3(a) shows an absorption spectrum measured for spherical Cu_xS nanoparticles with an average diameter of 5 nm.[29] Only a single plasmon peak is observed and no spectral component is present around 2 eV. This result indicates that the characteristic spectral peaks around 2 eV observed in the nanoplates are due to their anisotropic shapes. Figure 4 shows the energy positions estimated for both the in-plane and out-of-plane modes, plotted versus the aspect ratios of the nanoplates t/D. The energies of the out-of-plane mode are weakly dependent on the aspect ratios in contrast to those of the in-plane mode. Such spectral behavior is expected for CuS nanoplates from simulations based on full-wave time-harmonic finite element analysis.[20]

As is well known, the frequency position of the LSPR band depends on the dielectric environment of the nanoparticles.[1] The peak shift of the NIR absorption band has often been measured for Cu_xS nanoparticles dispersed in various organic solvents with different refractive indices (dielectric constants) to confirm that their NIR absorption band originates from the LSPR.[7,8,12,19] We also considered that investigating the effect of solvents on the absorption peak position provides strong evidence that the absorption peak around 2 eV was attributed to the LSPR. Thus, absorption spectra of the as-synthesized CuS nanoplates were measured after dispersing the samples in hexane, chloroform, carbon tetrachloride, toluene, and carbon dioxide. The refractive indices of these solvents are 1.38, 1.43, 1.46, 1.48, and 1.59, respectively. Figure 5 depicts the peak energies of the in-plane LSPR and the absorption peak around 2 eV (out-of-plane resonance) plotted versus the refractive indices

of the solvents. Both peaks exhibit similar red-shifts with an increase in the refractive indices of the solvents. Such tendencies have been expected for the observed LSPR. Therefore, we conclude that the weak absorption peak around 2 eV also originates from the LSPR and may be ascribed to the out-of-plane mode.

The LSPR of a nanoplate can be theoretically formulated by approximating it as an oblate spheroid. According to Gans' theory, the extinction coefficient of randomly oriented spheroidal particles with semiaxes a, b, and c is given by the following formula:[1,21]

$$\sigma_{ext}(\omega) = \frac{NV\omega\varepsilon_m^{3/2}}{3v} \sum_i \frac{\dfrac{\varepsilon_2(\omega)}{L_i^2}}{\left[\varepsilon_1(\omega) + \dfrac{1-L_i}{L_i}\varepsilon_m\right]^2 + \varepsilon_2(\omega)^2} \quad . \tag{1}$$

Here, N is the number of particles per unit volume, V the particle volume, ε_m the dielectric constant of a surrounding medium, ω the frequency of light, and v the speed of light. $\varepsilon_1(\omega)$ and $\varepsilon_2(\omega)$ are the real and imaginary parts of the complex dielectric function of the particles. L_i denotes the depolarization factors for the three principal axes (i $= x, y, z$), which are defined as follows for an oblate spheroid ($a = b > c$).[30]

$$L_x = L_y = \frac{g(e)}{2e^2}\left[\frac{\pi}{2} - \tan^{-1} g(e)\right] - \frac{g(e)^2}{2} \tag{2}$$

$$L_z = 1 - 2L_x \tag{3}$$

$$g(e) = \sqrt{\frac{1-e^2}{e^2}} \tag{4}$$

$$e^2 = 1 - \left(\frac{c}{a}\right)^2 \tag{5}$$

Here, the ratio c/a denotes the aspect ratio of the spheroidal particle, which corresponds to t/D defined for the CuS nanoplates in this work. The dielectric function of the particles can be represented by the Drude model as

$$\varepsilon(\omega) = 1 - \frac{\omega_p^2}{\omega^2 + i\Gamma\omega} \quad . \tag{6}$$

In this equation, ω_p and Γ are the plasma frequency and the damping constant of free carriers, respectively. The extinction spectrum can be represented by Eqs. (1)–(6) and approximated

by a Lorentzian function with a peak at ω_i and a FWHM of Γ_i which can be expressed as follows (Γ_i is equivalent to the damping constant of free carriers in a nanoparticle):

$$\omega_i = \sqrt{\frac{\omega_p^{\,2}}{1 + \dfrac{1 - L_i}{L_i}\varepsilon_m} - \Gamma_i^{\,2}} \quad . \tag{7}$$

Therefore, two resonant peaks, ω_x (= ω_y) and ω_z, arise for oblate spheroids which correspond to the in-plane and out-of-plane resonances in the nanoplates, respectively.

To quantitatively examine the position of the out-of-plane modes observed for the CuS nanoplates, we calculated the frequencies of the out-of-plane modes expected from this oblate-spheroid model. The Drude dielectric function given in Eq. (6) was used for this calculation because the dielectric function of CuS has so far not been provided experimentally with high reliability, especially not in the NIR region. Based on Eq. (7), the values of ω_p for nanoplates S1–S4 were extracted from the peak energies and FWHM of the in-plane LSPR bands and the depolarization factors L_x (= L_y), which were calculated by Eqs. (2)–(5) using the aspect ratios of the nanoplates. The dielectric constant of hexane was used for ε_m. Then, resonant energies of the out-of-plane modes were calculated by substituting the values of ω_p, L_z, and Γ_z into Eq. (7) again. Here, Γ_z values were obtained in the following way.

The damping constant of free carriers in a nanoparticle changes from its bulk value due to a limited carrier mean-free-path, and thus, depends on the nanoparticle size.[1] The damping constant for the bulk material, Γ_∞, is composed of contributions from carrier-carrier, carrier-phonon, and carrier-defect scattering. In nanoparticles with diameters less than the mean-free-path, an additional scattering process via collision with the nanoparticle surface becomes dominant. Therefore, the damping constant of a nanoparticle with a diameter D can be expressed as follows:[1]

$$\Gamma(D) = \Gamma_\infty + 2\frac{v_F}{D} \quad . \tag{8}$$

Here, v_F is the Fermi velocity. Such a size-dependence of the damping constant can be confirmed for the in-plane mode of the CuS nanoplates, as shown in Fig. 2(b). The values of the FWHM of the in-plane mode, which are equivalent to the damping constant, are proportional to the reciprocal nanoplate diameter, exhibiting the tendency indicated by Eq.

(8). The damping constants of carriers in the out-of-plane direction (i.e., traversing the plate thickness), which corresponds to Γ_z, could be estimated from the relation determined for the in-plane mode by linear fitting using the least-square method [dashed line in Fig. 2(b)]. By the use of thickness t as an alternative to the diameter in Eq. (8), the damping constant in the thickness direction was calculated. Finally, the resonance frequencies of the out-of-plane mode, ω_z^{calc}, were deduced for nanoplates S1–S4. The parameters used in these calculations and estimated values of ω_z^{calc} are summarized in Table I. Values of ω_z^{calc} are close to the peak energies of the out-of-plane mode, ~2 eV. There are some differences between calculated and measured values, which could be attributed to deviations in the shape of actual CuS nanoplates from that of an oblate spheroid. Consequently, we conclude that the weak absorption peak around 2 eV found for the CuS nanoplates in this study is ascribable to the out-of-plane mode of the LSPR. The out-of-plane LSPR was experimentally identified for size-selected CuS nanoplates, while theoretical calculations indicated that this mode is challenging to observe due to its low intensity and overlap with the strong in-plane LSPR band.

4. Conclusions

Plate-shaped CuS nanoparticles with covellite structure were synthesized by a standard heat-up method. A size-selective precipitation technique was adopted and the CuS nanoplates were successfully separated into four fractions with different aspect ratios. The strong NIR absorption bands ascribed to the in-plane mode of the LSPR were the dominant spectral features in samples from all fractions. In addition, we found a weak absorption peak on the high energy side of the in-plane mode in all the nanoplate samples, which so far has not been reported for CuS nanoplates. Reasonable agreement in spectral features, including a strong in-plane mode and a very weak out-of-plane mode, was found between the experimental spectra and calculated spectra, simulated for CuS nanoplates in a previous study.[19] By an analysis of the peak positions of the nanoplates for different dielectric environments, their aspect ratio dependence, and calculations of resonance frequencies of the LSPR based on Gans' theory, these additional peaks could be assigned to the out-of-plane mode.

Acknowledgments

References

1) R. Kreibig and M. Vollmer, *Optical Properties of Metal Clusters* (Springer, Berlin, 1995).

2) G. Mie, Ann. Phys. (Berlin) **25**, 377 (1908) [in German].

3) D. Thompson, Gold Bull. **40**, 267 (2007).

4) S. A. Maier, *Plasmonics: Fundamentals and Application* (Springer, New York, 2007)

5) M. Pelton and G. W. Bryant, *Introduction to Metal-Nanoparticle Plasmonics* (Wiley, Hoboken, NJ, 2013).

6) Y. Zhao, H. Pan, Y. Lou, X. Qiu, J. Zhu, and C. Burda, J. Am. Chem. Soc. **131**, 4253 (2009).

7) M. Kanehara, H. Koike, T. Yoshinaga, and T. Teranishi, J. Am. Chem. Soc. **131**, 17736 (2009).

8) J. M. Luther, P. K. Jain, T. Ewers, and A. P. Alivisatos, Nat. Mater. **10**, 361 (2011).

9) R. Buonsanti, A. Llordes, S. Aloni, B. A. Helms, and D. J. Milliron, Nano Lett. **11**, 4706 (2011).

10) D. J. Rowe, J. S. Jeong, K. A. Mkhoyan, and U. R. Kortshagen, Nano Lett. **13**, 1317 (2013).

11) C. M. Hessel, V. P. Pattani, M. Rasch, M. G. Panthani, B. Koo, J. W. Tunnell, B. A. Korgel, Nano Lett. **11**, 2560 (2011).

12) H. Nishi, K. Asami, and T. Tatsuma, Opt. Mater. Express **6**, 1043 (2016).

13) I. Kriegel, J. Rodriguez-Fernández, A. Wisnet, H. Zhang, C. Waurisch, A. Eychmüller, A. Dubavik, A. O. Govorov, and J. Feldman, ACS Nano **7**, 4367 (2013).

14) V. V. Gorbachev and I. M. Putilin, Phys. Status Solidi A **16**, 553 (1973).

15) P. Lukashev and W. R. L. Lambrecht, Phys. Rev. B **76**, 195202 (2007).

16) S. W. Hsu, K. On, and A. R. Tao, J. Am. Chem. Soc. **133**, 19072 (2011).

17) T. Wei, Y. Liu, W. Dong, Y. Zhang, C. Huang, Y. Sun, X. Chen, and N. Dai, ACS Appl. Mater. Interface **5**, 10473 (2013).

18) G. Manna, R. Bose, and N. Pradhan, Angew. Chem., Int. Ed. **52**, 6762 (2013).

19) Y. Xie, L. Cabone, C. Nobile, V. Grillo, S. D'Agostino, F. D. Sala, C. Giannini, D. Altamura, C. Oelsner, C. Kryshi, and P. D. Cozzoli, ACS Nano **7**, 7352 (2013).

20) M. Liu, X. Xue, C. Ghosh, X. Liu, Y. Liu, E. P. Furlani, M. T. Swihart, and P. N. Prasad, Chem. Mater. **27**, 2584 (2015).

21) S. Link, M. B. Mohamed, and M. A. El-Sayed, J. Phys. Chem. B **103**, 3073 (1999).

22) R. Jin, Y. W. Cao, C. A. Mirkin, K. L. Kelly, G. C. Schatz, and J. G. Zheng, Science **294**, 1901 (2001).

23) W. Li, R. Zamani, P. R. Gil, B. Pelaz, M. Ibáñez, D. Cadavid, A. Shavel, R. A. Alvarez-Puebla, W. J. Parak, J. Arbiol, and A. Cabot, J. Am. Chem. Soc. **135**, 7098 (2013).

24) R. Jin, Y. C. Cao, E. Hao, S. Métraux, G. C. Schatz, and C. A. Mirkin, Nature 425, 487 (2003).

25) E. Hao, G. C. Schatz, and J. T. Hupp, J. Fluoresc. **14**, 331 (2004).

26) L. Vossmeyer, L. Katsikas, M. Giersig, I. G. Popovic, K. Diesner, A. Chemseddine, A. Eychmüller, and H. Weller, J. Phys. Chem. **98**, 7665 (1994).

27) R. L. Whetten, J. T. Khoury, M. M. Alvarez, S. Murthy, I. Vezmar, Z. L. Wang, P. W. Stephens, C. L. Cleveland, W. D. Luedtke, and U. Landman, Adv. Mater. **8**, 428 (1996).

28) S. W. Hsu, C. Ngo, and A. R. Tao, Nano Lett. **14**, 2372 (2014).

29) Y. Hamanaka, T. Hirose, K. Yamada, and T Kuzuya, Opt. Mater. Express **6**, 3838 (2016).

30) C. F. Bohren and D. R. Hoffman, *Absorption and Scattering of Light by Small Particles* (Wiley-VCH, Weinheim, 2004).

Figure Captions

Fig. 1. (Color online) TEM images of the CuS nanoplates: (a) S1, (b) S2, (c) S3, and (d) S4. (e) XRD pattern of the CuS nanoplates before the size selection and JCPDS pattern of the hexagonal CuS.

Fig. 2. (Color online) (a) Absorption spectra of size-selected CuS nanoplates S1–S4. (b) FWHM of the LSPR absorption bands of the size-selected CuS nanoplates S1–S4.

Fig. 3. (Color online) (a) Absorption spectra and (b)–(e) secondary differential spectra of size-selected CuS nanoplates S1–S4, respectively. The inset displays the absorption spectrum of the Cu_xS nanospheres with an average diameter of 5 nm, as reported in Ref. 29.

Fig. 4. (Color online) Peak energies of the in-plane (circles) and out-of-plane (triangles) modes of the LSPR of size-selected CuS nanoplates S1–S4 with different aspect ratios *t/D*.

Fig. 5. (Color online) Energies of the LSPR measured for CuS nanoplates dispersed in various organic solvents with different refractive indices. (a) Out-of-plane mode. (b) In-plane mode.

Table I. Geometrical parameters and parameters of the LSPR bands of CuS nanoplates.

Sample	D (nm)	t (nm)	Aspect ratio	In-plane mode		ω_p (eV)	Out-of-plane mode		
				ω_x (eV)	Γ_x (eV)		ω_z (eV)	Γ_z (eV)	ω_z^{calc} (eV)
S1	17.1	5	0.29	0.957	0.373	3.322	2.00 ± 0.05	0.617	2.302
S2	13.5	4	0.30	0.985	0.428	3.454	2.00 ± 0.05	0.698	2.368
S3	11.6	4	0.35	1.052	0.448	3.471	1.99 ± 0.05	0.698	2.273
S4	8.7	4	0.46	1.116	0.469	3.322	2.01 ± 0.05	0.698	1.964

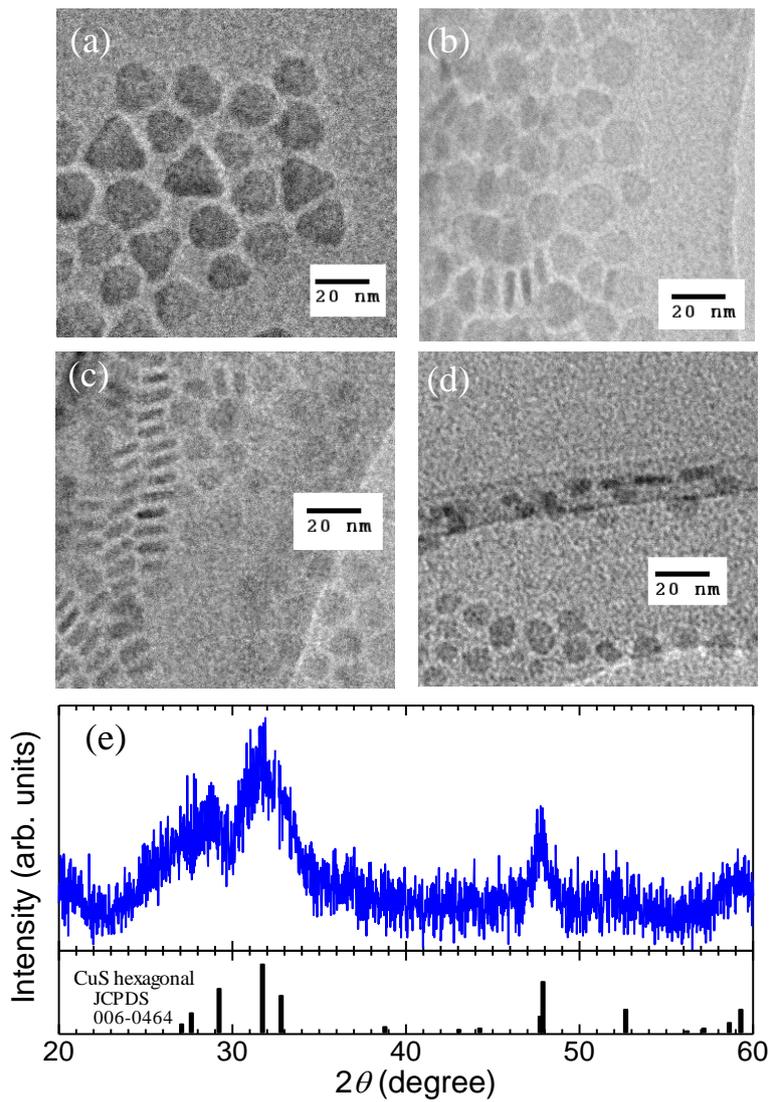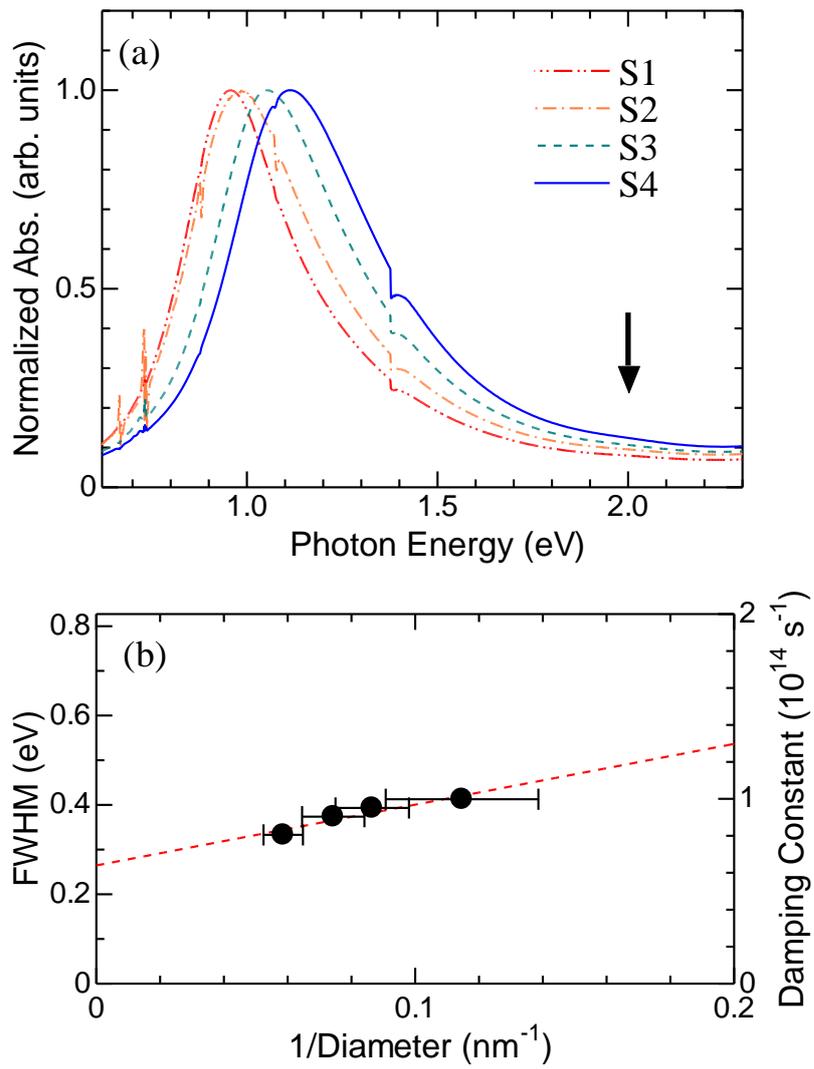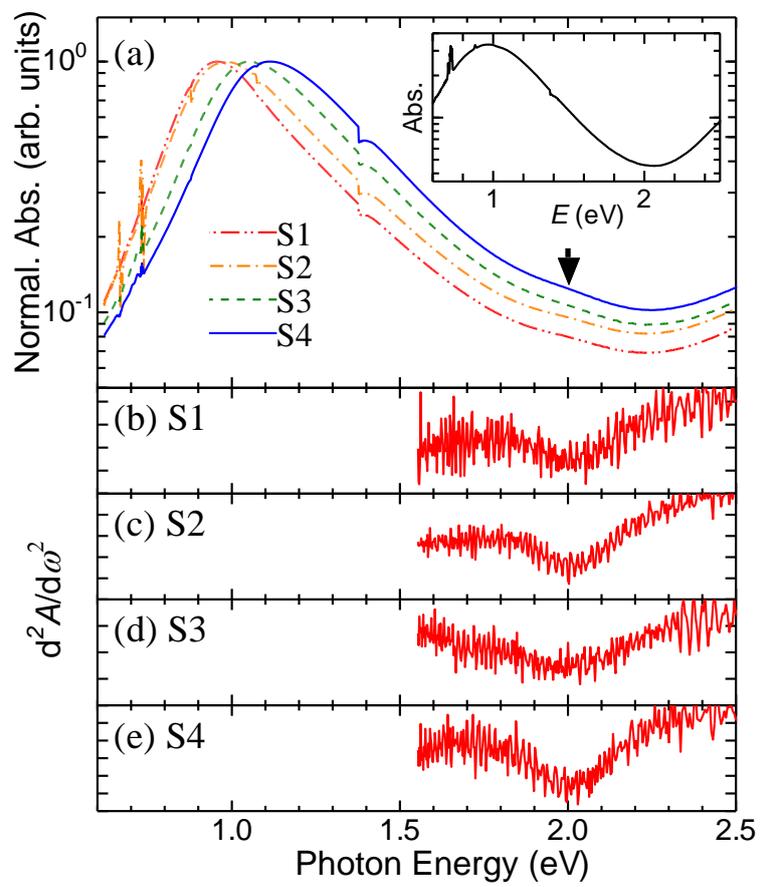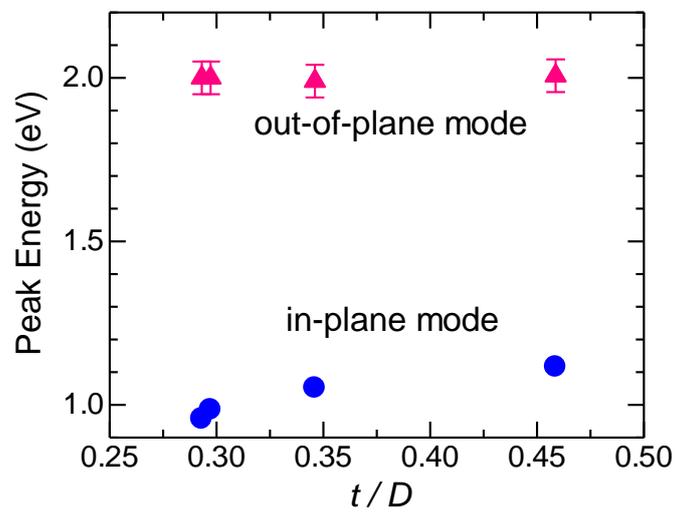Fig. 1 Y. Hamanaka et al.

Fig. 2 Y. Hamanaka et al.

Fig. 3 Y. Hamanaka et al.

Fig. 4 Y. Hamanaka et al.

Fig. 5 Y. Hamanaka et al.